

# Neutron Form Factors from High-Energy Inelastic Electron-Deuteron Scattering\*

S. SOBOTKA†

*Department of Physics and High-Energy Physics Laboratory, Stanford University, Stanford, California*

(Received November 30, 1959)

The inelastic electron-deuteron scattering cross section has been measured for incident electron energies between 300 Mev and 650 Mev and for final electron energies primarily at the maxima of the inelastic continua. The data were interpreted in terms of neutron form factors by employing the impulse approximation calculations of Goldberg. The results indicate that  $F_{2n}^2$  is nearly equal to the proton form factor  $F_p^2$  for  $2.65 < q^2 < 15.1$  (fermi)<sup>-2</sup> but may be 20% or 30% higher than  $F_p^2$  for the lowest of these  $q$  values. Uncertainties, primarily in the theory, make it impossible to determine whether the difference is real. The results also indicate that  $-2.5 < F_{1n}/F_{2n} < 0.5$  for  $5.1 < q^2 < 12.8$  f<sup>-2</sup>.

## I. INTRODUCTION

IT is possible to learn about the electromagnetic properties of the neutron by scattering high-energy electrons from deuterium and by detecting those electrons which have scattered after breaking up the deuteron into free nucleons. In this experiment, attention was directed to the peak of inelastic continua measured as a function of final electron energy, for incident energies between 300 and 650 Mev. In addition, a few measurements were made of the cross section for essentially all final electron energies corresponding to deuteron breakup, in order to compare the shape of the cross-section curve with the theory of Jankus<sup>1</sup> for low values of the four-momentum transfer  $q$ .

Yearian and Hofstadter<sup>2</sup> have previously measured the cross section for deuteron breakup for incident electron energies of 500 and 600 Mev. The cross sections, integrated over final electron energies, were interpreted in terms of the theories of Jankus<sup>1</sup> (with modifications described in reference 2) and of Blankenbecler.<sup>3</sup> The cross sections for final electron energies at the maximum were interpreted in terms of the modified Jankus theory.<sup>2</sup> In the analysis, the above authors assumed  $F_{1n}^2 = 0$  and determined  $F_{2n}^2$ . They found that  $F_{2n}^2$  was about the same as  $F_p^2$ , the proton form factor<sup>4</sup> squared, and that an exponential density distribution with a rms radius of  $0.76 \pm 0.1$  fermi led to a form factor which agreed with their data.

In the present work the data are considerably improved and the analysis was done with the aid of the impulse approximation calculations of Goldberg.<sup>5</sup> Initially,  $F_{1n}$  was assumed to equal zero in order to find  $F_{2n}^2$ . Upper limits were also placed on  $F_{1n}/F_{2n}$  by

making measurements at both large and small angles with the incident energy adjusted to give the same value of  $q$ .

## II. THEORY

Goldberg<sup>5</sup> used the impulse approximation to calculate the cross section, thus assuming it to be the sum of the cross sections for two free nucleons with a momentum distribution derived from a <sup>3</sup>S deuteron ground-state wave function. The nucleons were also assumed to be unbound in the final state. Since then, Goldberg has extended the calculation to include the <sup>3</sup>D state as well.<sup>6</sup> The values of  $d^2\sigma/d\Omega dE'$ , where  $E'$  is the final electron energy, for  $E'$  taken at the maximum of the inelastic continua were within 6% of those predicted by the modified Jankus theory. Goldberg's expression for the cross section included the integrals

$$I_1 = \int_b^\infty \epsilon^2 F_u^2(p) d\epsilon,$$

$$I_2 = \int_b^\infty \epsilon F_u^2(p) d\epsilon,$$

and

$$I_3 = \int_b^\infty F_u^2(p) d\epsilon,$$

where  $p$  is the relative momentum of the nucleons in the deuteron,  $\epsilon$  is the relativistic energy corresponding to  $p$ ,

$$b = \hbar c \left\{ \frac{-q_0}{2} + \frac{1}{2} \left[ q^2 \left( 1 - \frac{4M^2 c^2}{\hbar^2 q^2} \right) \right]^{1/2} \right\},$$

$q_0$  is the time-like part of  $q$ ,  $\mathbf{q}$  is the vector spatial part,  $M$  is the nucleon mass,

$$F_u = \left( \frac{2}{\pi} \right)^{1/2} \int_0^\infty u(r) j_0(pr) r dr,$$

$u(r)$  is the radial  $S$ -state deuteron wave function with

\* Supported by the joint program of the Office of Naval Research, the Atomic Energy Commission, and the Air Force Office of Scientific Research.

† Now at Boeing Scientific Research Laboratories, Boeing Aircraft Company, Seattle, Washington.

<sup>1</sup> V. Z. Jankus, Phys. Rev. **102**, 1586 (1956).

<sup>2</sup> M. R. Yearian and R. Hofstadter, Phys. Rev. **110**, 552 (1958); **111**, 934 (1958).

<sup>3</sup> R. Blankenbecler, Phys. Rev. **111**, 1684 (1958).

<sup>4</sup> See R. Hofstadter, F. Bumiller, and M. R. Yearian, Revs. Modern Phys. **30**, 482 (1958), for a review of the experiments on the proton.

<sup>5</sup> A. Goldberg, Phys. Rev. **112**, 618 (1958).

<sup>6</sup> A. Goldberg (private communication).

normalization such that

$$4\pi \int_0^\infty u^2(r) dr = 1,$$

and  $j_0$  is the zeroth order spherical Bessel function. When the deuteron  $D$  state is included, the sole changes are to replace the integrals above with

$$I_1 = \int_b^\infty \epsilon^2 [F_u^2(p) + (1/\sqrt{8})F_u(p)F_w(p) + (9/32)F_w^2(p)] d\epsilon,$$

$$I_2 = \int_b^\infty \epsilon [F_u^2 + (1/\sqrt{8})F_u F_w + (9/32)F_w^2] d\epsilon,$$

$$I_3 = \int_b^\infty [F_u^2 + (1/\sqrt{8})F_u F_w + (9/32)F_w^2] d\epsilon,$$

where

$$F_w(p) = \left(\frac{2}{\pi}\right)^{\frac{1}{2}} \int_0^\infty w(r) j_2(pr) r dr,$$

and where  $w$  is the radial  $D$ -state deuteron wave function and the normalization is now such that

$$4\pi \int_0^\infty [u^2(r) + w^2(r)] dr = 1.$$

Goldberg has also shown that the peak cross section is proportional, within about 3%, to the sum of the Rosenbluth<sup>7</sup> cross sections for electron scattering from a free neutron and a free proton. He also showed that the deuteron dependence in the peak cross section was primarily multiplicative and independent of incident electron energy and other such parameters.

Goldberg's complete expression for the cross section was used by the present author to calculate the peak cross sections on an IBM 650 computer for three different wave functions:

- (a) The Hulthén<sup>8</sup>  $S$ -state wave function,
- (b) The Rustgi<sup>9</sup>  $S$ -state wave function,
- (c) Analytic approximations to the Gartenhaus<sup>10</sup>  $S$ - and  $D$ -state wave functions. The  $S$ -state approximation of case (c) was one constructed by Moravcsik,<sup>11</sup> while the  $D$ -state approximation was constructed by the present author and designed to simplify the calculation of  $F_w$ . The ratios of the peak heights with these three wave functions were 1.00:1.02:0.98, respectively. The

<sup>7</sup> M. N. Rosenbluth, Phys. Rev. **79**, 615 (1950).

<sup>8</sup> The Hulthén wave function was that used by Jankus. See reference 1.

<sup>9</sup> M. L. Rustgi, Rev. mex. fis. **6**, 135 (1957).

<sup>10</sup> S. Gartenhaus, Phys. Rev. **100**, 900 (1955).

<sup>11</sup> M. J. Moravcsik (unpublished). However, see M. J. Moravcsik, Nuclear Phys. **7**, 113 (1958), for similar approximations.

terms in  $I_1$ ,  $I_2$ ,  $I_3$  involving  $w$  produced negligible contributions to the peak height in case (c).

A calculation was also made of the complete spectrum at 500 Mev, 60°, for the Gartenhaus wave functions and compared to that for the Hulthén wave function. The result is shown in Fig. 1. Also shown is the result of a calculation including all but the first term in each of  $I_1$ ,  $I_2$ ,  $I_3$ , using the Gartenhaus wave functions in order to show the  $D$ -state contributions.

The uncertainty in the peak cross sections is thus about 2% due to the uncertainty in the deuteron wave function. In the present analysis, the Hulthén wave function was used.

Other uncertainties in the theoretical peak cross section result from the neglected final-state interaction, neutron-proton interference terms, and meson-exchange contributions. Durand<sup>12</sup> has estimated that at 500 Mev, 75°, there may be a 5 or 10% contribution from the first and 1 or 2% from the third. For no final-state interaction, the interference terms are less than 1% as calculated from a semirelativistic expression for the cross section given by Durand, although these terms will probably be larger with a final state interaction.

The conclusion is that if Durand's calculations are taken seriously the theoretical peak cross section (at 500 Mev, 75°) is in doubt by 5 or 10%, and since the peak section is proportional to the sum of the elastic neutron and proton cross sections, it will be seen that the error in the experimental neutron cross sections of this work may be from 3 to 6 times as large.

### III. EXPERIMENTAL APPARATUS AND PROCEDURE

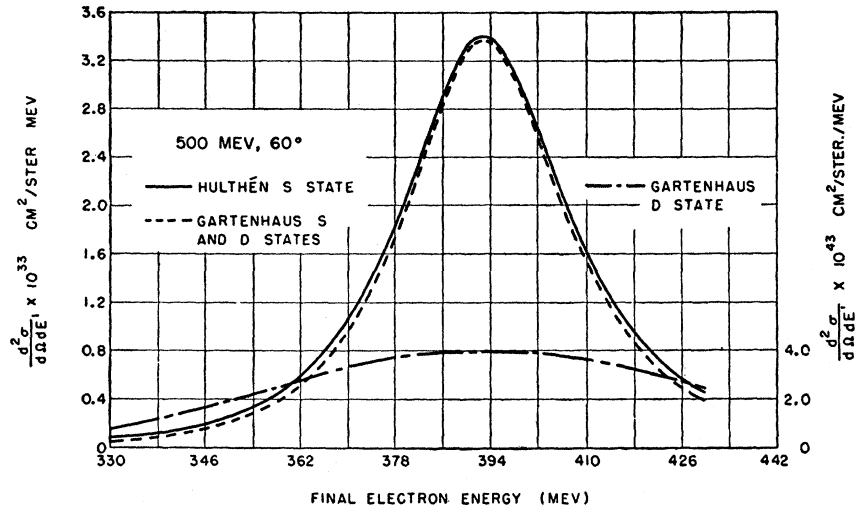
The apparatus was largely that used in previous electron-scattering experiments.<sup>13</sup> The peak-height data were taken with a liquid target having a radiation length only about  $\frac{2}{3}$  of that previously used,<sup>2</sup> so the radiation corrections are smaller. Over-all energy resolution figures for these data were about 2½%, necessitating resolution corrections to the deuteron data but rendering the elastic hydrogen normalizing data reasonably insensitive to instrumental fluctuations.

Absolute cross sections were made possible by measuring the elastic proton cross section at each incident electron energy and scattering angle and normalizing with the calculated proton cross section using the exponential model of radius 0.8 f shown to be valid by Chambers and Hofstadter and by Hofstadter, Bumiller, and Yearian.<sup>4</sup> Instrumental errors were minimized by measuring both the deuteron and proton data during the same runs. The statistical accuracy of the deuteron data was usually between 2 and 3% although a low counting rate and large  $\pi^-$  backgrounds at a couple of the points produced larger uncertainties. The relative accuracy of the proton data was judged to

<sup>12</sup> L. Durand, III, Phys. Rev. **115**, 1020 (1959).

<sup>13</sup> R. Hofstadter, Revs. Modern Phys. **28**, 214 (1956).

FIG. 1. Impulse approximation calculations of the cross section at 500 Mev, 60°, using Hulthén and Gartenhaus wave functions (left-hand ordinate axis). The *D*-state contribution for the Gartenhaus wave function is also plotted (right-hand ordinate axis).



be about 3% although the standard deviations calculated from the number of counts were between 1 and 2%. The proton data were useful only for normalizing purposes since no attempt was made to maintain counting efficiencies independent of incident energy and scattering angle.

#### IV. CORRECTIONS TO THE DATA

The radiation corrections were calculated using the following energy spectrum for electrons which radiated before and after scattering from a nucleon:

$$v(E_0, E_4, E') dE' = \frac{(1 + \frac{3}{2}s)}{\Gamma(y + y' + 1)} \left( \frac{E_0}{E_0'} \right)^y E_0'^{-y} E_4^{-y'} \times (E_4 - E')^{y+y'-1} \left\{ y \left[ \frac{1}{2} + \frac{1}{2} \left( \frac{E_3}{E_0} \right)^2 \right] \sigma(E_3) + y' \left[ \frac{1}{2} + \frac{1}{2} \left( \frac{E'}{E_4} \right)^2 \right] \sigma(E_0) \right\} dE', \quad (1)$$

where  $E_0$  is the initial electron energy and  $E_0'$  is the corresponding final energy for elastic scattering,  $E_3$  is the initial energy corresponding to an elastic peak at  $E_0' - (E_4 - E')$ ,  $E'$  is the final electron energy,  $s = (2\alpha/\pi) [\ln(\hbar q/mc) - \frac{1}{2}]$  where  $m$  is the electron mass,  $y = bx + s$  where  $b = 1/0.739T$  and  $T$  is one radiation thickness of the target medium,  $x$  is the target thickness in cm before scattering,  $y' = bx' + s$  where  $x'$  is the target thickness after scattering. The origin of Eq. (1) is given in the Appendix. It combines the probabilities for radiation in the target medium before and after scattering with the probability for radiating at the time of scattering. The latter results from the Schwinger correction<sup>14</sup> and wide-angle bremsstrahlung formula.<sup>15</sup>

<sup>14</sup> J. Schwinger, Phys. Rev. **75**, 899 (1949). See also, D. R. Yennie and H. Suura, Phys. Rev. **105**, 1378 (1957).

<sup>15</sup> W. K. H. Panofsky and E. A. Allton, Phys. Rev. **110**, 1155

Equation (1) is precise in the limit of small energy losses and is accurate to about 10% for energy losses of half of the incident energy. The elastic proton peaks were measured only for energies down to  $0.95E_0'$  and the remaining cross section was calculated by letting  $E_4 = E_0'$  in Eq. (1) and integrating for  $E'$  between  $E_0'$  and  $0.95E_0'$ . The radiation corrections to the deuteron peak-height data were calculated by a method equivalent to evaluating the integral

$$v_{in}(E_0, E') dE' = dE' \int_{E'}^{E_0} \left( \frac{d^2\sigma}{d\Omega dE_4} \right) v(E_0, E_4, E') dE_4, \quad (2)$$

where  $E'$  is equal to the energy at the cross-section maximum and  $v_{in}(E_0, E')$  is the observed cross section (neglecting other than radiative corrections). Equation (1) was also used to calculate the magnitude of the radiative tail of the elastic deuteron peak at the inelastic maximum; this tail was found to be negligible. The radiation corrections to the complete deuteron spectra were calculated by using a numerical procedure which yielded  $d^2\sigma/d\Omega dE_4$  of Eq. (2) for any  $E_4$  in the spectrum. The correction applied to the peak-height data was the ratio of the correction for the deuteron peak to that of the proton peak. This ratio varied between 1.035 at 350 Mev, 60°, and 0.980 at 300 Mev, 135°. Individually, the proton peak- and deuteron peak-height corrections were between 15 and 20%.

A negative meson background was observed and was calculated by multiplying the measured  $\pi^+$  counting rate by the  $\pi^-/\pi^+$  cross-section ratio,<sup>16,17</sup> and then was subtracted from the data. Energy resolution corrections varied between 1.3% at 500 Mev, 135°, and 5.9% at

(1958). These authors used integrals evaluated in L. I. Schiff, Phys. Rev. **87**, 750 (1952).

<sup>16</sup> M. Sands, J. G. Teasdale, and R. L. Walker, Phys. Rev. **95**, 592 (1954). See also K. M. Watson, J. C. Keck, A. V. Tollestrup, and R. L. Walker, Phys. Rev. **101**, 1159 (1956).

<sup>17</sup> G. Neugebauer, W. D. Wales, and R. L. Walker, Phys. Rev. Letters **2**, 429 (1959).

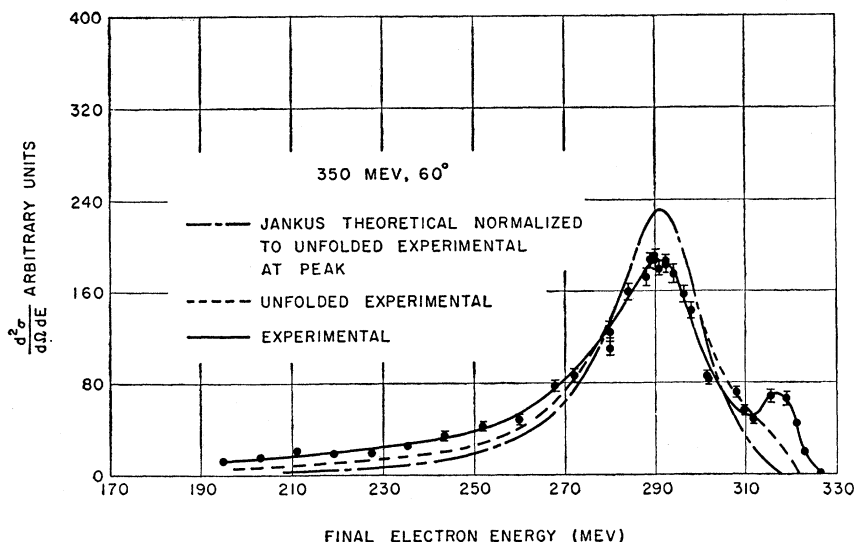


FIG. 2. Experimental cross section at 350 Mev, 60°, compared to the modified Jankus theoretical curve. The "Unfolded Experimental" is the radiation-corrected experimental curve. The Jankus theoretical curve is normalized to the latter at the maximum. These two curves do not include the elastic peak at the right on the experimental curve.

500 Mev, 60°, and were applied to the peak-height data. Angular resolution corrections were unnecessary because calculations showed that they cancelled with negligible error in the ratio of deuteron to proton cross section. Counting rate corrections to account for the fact that the counting apparatus could record no more than one count per incident beam pulse were applied and were always less than 6%. The larger corrections occurred at smaller angles. The usual correction was applied accounting for the fact that the spectrometer dispersion is a function of the energy. The difference between the atomic densities of the deuterium and the

hydrogen was taken into account in normalizing the data. The proton contamination of the deuterium was found to be between 0.4 and 0.5% by mass spectrographic analysis and because of this a 1% correction was made to the peak-height data. A correction of up to 5% was applied to the complete spectrum at 600 Mev, 55° to correct for the variation in effective solid angle of the spectrometer at the large values of magnetic field where a certain amount of saturation occurs.

The total uncertainty in the peak cross section resulting from the uncertainty of the corrections is probably no more than 2%.

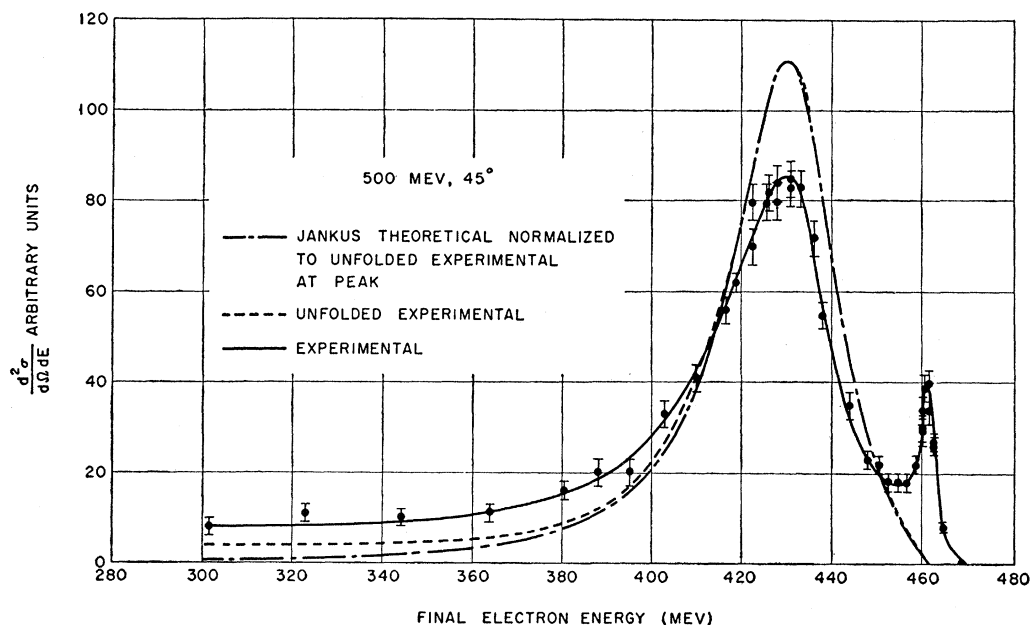
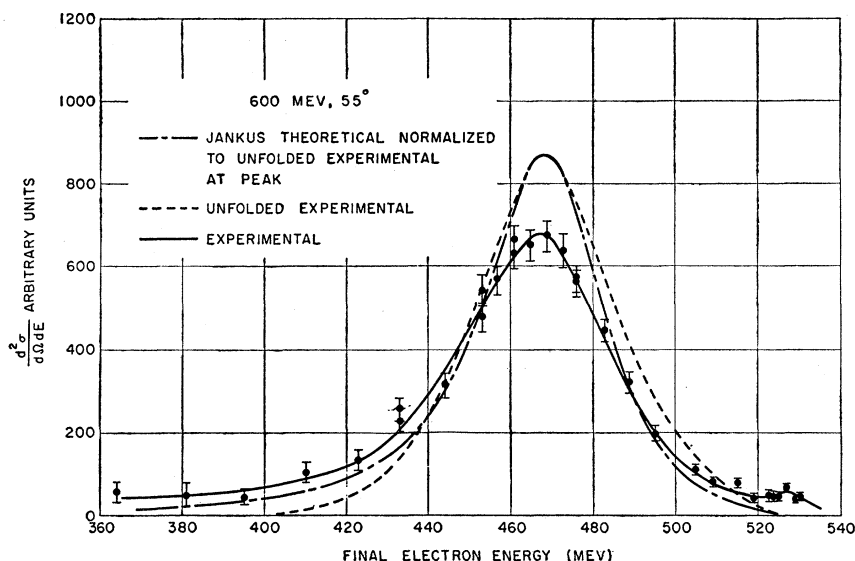


FIG. 3. Experimental cross section at 500 Mev, 45°, compared to the modified Jankus theoretical curve. The "Unfolded Experimental" is the radiation-corrected experimental curve. The Jankus theoretical curve is normalized to the latter at the maximum. These two curves do not include the elastic peak at the right on the experimental curve.

Fig. 4. Experimental cross section at 600 Mev, 55°, compared to the modified Jankus theoretical curve. The "Unfolded Experimental" is the radiation-corrected experimental curve. The Jankus theoretical curve is normalized to the latter at the maximum. These two curves do not include the elastic peak at the right on the experimental curve.



The radiative corrections produced larger errors in the complete spectra than in the peak-height results because of errors in the numerical method and errors in Eq. (1) for large radiative energy losses. The corrections are accurate to about 2 or 3% for points near the maxima and on the high-energy sides of the maxima. For points at lower energies, the accuracy becomes increasingly poor. Points with counting rates higher than 20% of the maxima have errors less than about 10% but the errors may be as large as 50% in the low-energy tails. No absolute cross sections were deduced from such data. The complete curves are used only to compare their spectral shapes with those predicted by the Jankus theory.

#### V. EXPERIMENTAL DATA AND ANALYSIS

Figures 2, 3, and 4 show three inelastic spectra, two of which are at lower  $q$  values than those reached by Yearian and Hofstadter. The 350 Mev, 60°, curve was measured with the new target, while the other two were measured with the old target. These data have somewhat larger statistical errors than the peak-height data. The curve at 600 Mev, 55°, has about the same half-width as all those measured by Yearian and Hofstadter. The experimental curves were drawn by eye through the data points, which had received all corrections except the radiative correction. A rough subtraction of the elastic data was then made and the radiative corrections applied to the remainder, resulting in the unfolded experimental curves. These curves are rather inaccurate in the region of the elastic peak because of the low resolution and the crudeness of the subtraction. The theoretical curves were calculated on an IBM 707 computer by R. Herman from the modified Jankus theory.<sup>2</sup> The theoretical and unfolded experimental curves are normalized together at the peak in order to facilitate comparison of the spectrum shapes. It is seen

that, for the low  $q$  values, the agreement is reasonably good. As  $q$  increases, however, the experimental curves become wider than the theoretical ones so that the unfolded curve at 600 Mev, 55°, is about 5 Mev wider than the theoretical. Some of the discrepancy in width would be removed if comparison had been made with the impulse approximation calculations.<sup>5</sup> Also, inclusion of the final-state interaction would widen the curves somewhat although the effect is expected to diminish as  $q$  increases.

The experimental full widths at half maximum are seen to vary from about 28 Mev at 350 Mev, 60°, to about 44 Mev at 600 Mev, 55°, while the unfolded experimental widths vary from about 25 Mev to 39 Mev.

TABLE I. Experimental values of the deuteron cross section at the maxima of the inelastic continua. The uncertainties given are statistical.

Energy (Mev)	Angle (degrees)	$(d^2\sigma/d\Omega dE)_{\max} \times 10^{34}$ (cm <sup>2</sup> /sr Mev)	Uncertainty (%)
300	105	17.5	4.2
300	135	8.32	4.4
350	60	121	3.9
350	135	5.16	3.6
425	135	2.85	3.9
450	135	2.21	4.2
500	60	35.8	3.8
500	60	36.0	3.7
500	135	1.45	3.8
550	75	8.66	5.2
550	135	1.16	4.3
550	135	1.02	5.1
600	60	17.9	4.2
600	60	17.7	3.7
600	75	5.82	4.0
600	75	5.81	3.9
600	90	2.89	4.3
600	135	0.770	4.9
650	90	2.00	6.1

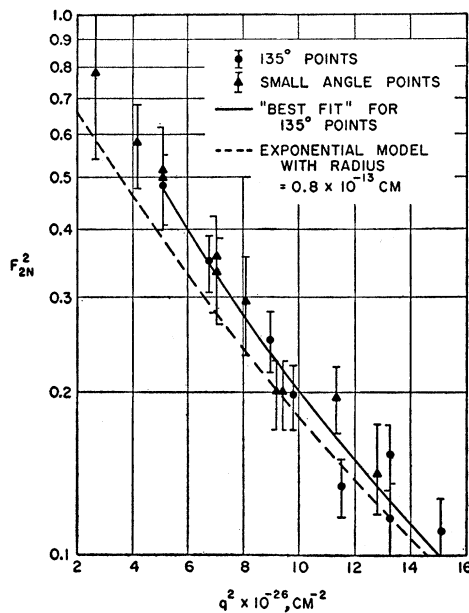


FIG. 5.  $F_{2n}^2$  assuming  $F_{1n}=0$ . The triangles refer to the small angle points, and the circles refer to the  $135^\circ$  points. The dotted line represents  $F_p^2$  and the solid line is a line drawn by eye through the  $135^\circ$  points for interpolation purposes.

The results of the peak-height measurements are given in Table I. The uncertainties quoted are statistical. An additional uncertainty is introduced by the 10% possible error in the calculated proton cross section<sup>4</sup> used to normalize the data. It is believed that all other uncertainties associated with this experiment do not total more than about 3%.

The data were first analyzed assuming  $F_{1n}=0$  and the results are shown in Fig. 5 and Table II. We see that  $F_{2n}^2$  is about equal to  $F_p^2$  for the large  $q$  values but appears to be 25 or 35% larger than  $F_p^2$  at the low  $q$  values. It is impossible at this time to tell whether this difference is real for several reasons. An increase of about 6 or 8% in the theoretical cross section at low  $q$  values would remove the difference. The calculations done to date by Durand<sup>12</sup> and by Jankus<sup>1</sup> indicated that the corrections due to final state interaction would decrease the cross section, and if this is actually the case, the difference between  $F_{2n}^2$  and  $F_p^2$  would become even greater. However, the calculations probably are too rough to preclude an increase in the cross section due to final state interaction.

$$R = \frac{\{Y^2 + (\hbar^2 q^2 / 4M^2 c^2) [2(Y + K_n)^2 \tan^2(\theta_s/2) + K_n^2]\} [2 \tan^2(\theta_L/2) + 1]}{\{Y^2 + (\hbar^2 q^2 / 4M^2 c^2) [2(Y + K_n)^2 \tan^2(\theta_L/2) + K_n^2]\} [2 \tan^2(\theta_s/2) + 1]} \quad (3)$$

where  $M$  is the nucleon mass and  $K_n$  is the neutron magnetic moment in nuclear magnetons.  $F_{2n}^2$  for  $\theta_L$  was interpolated *via* the solid line connecting the  $135^\circ$  points in Fig. 5. Figure 6 shows the values of  $Y$  resulting from solving Eq. (3) for  $Y$ . The values of  $Y$  at the theoretical minimum of  $R$  were chosen when the experimental values of  $R$  led to an imaginary  $Y$ .

TABLE II. Experimental values of the neutron magnetic form factor squared. The uncertainties are statistical.

Energy (Mev)	Angle (degrees)	$q^2 \times 10^{-26}$ (cm <sup>-2</sup> )	$F_{2n}^2$	Uncertainty (%)
300	105	4.15	0.580	15
300	135	5.11	0.479	13
350	60	2.65	0.782	26
350	135	6.56	0.348	10
425	135	8.92	0.250	12
450	135	9.76	0.198	13
500	60	5.08	0.498	17
500	60	5.08	0.516	17
500	135	11.48	0.134	12
550	75	8.04	0.295	18
550	135	13.26	0.153	14
550	135	13.26	0.117	16
600	60	7.02	0.351	16
600	60	7.02	0.329	14
600	75	9.31	0.199	14
600	75	9.31	0.199	13
600	90	11.30	0.196	15
600	135	15.09	0.111	16
650	90	12.84	0.147	19

Another uncertainty results from the unknown magnitude of  $F_{1n}$ . However, the limits placed on  $F_{1n}$  by the elastic scattering experiments of McIntyre et al.<sup>18</sup> and by the neutron-electron interaction experiments<sup>19</sup> show that this error is only about 2% in  $F_{2n}^2$  at  $q^2=3 \text{ f}^{-2}$ , 4% at  $q^2=5 \text{ f}^{-2}$  and 9% at  $q^2=8 \text{ f}^{-2}$ .

Also, the uncertainty in the calculated value of the proton cross section produces an equal uncertainty in the measured values of  $F_{2n}^2$ . Thus there are several possible sources of error in  $F_{2n}^2$ , the primary one corresponding to a theoretical uncertainty. The aggregate error could be large enough to remove the difference between  $F_{2n}^2$  and  $F_p^2$ .

As Fig. 5 indicates, data were taken at both small angles ( $60^\circ$ ,  $75^\circ$ , and  $90^\circ$ ) and at a large angle ( $135^\circ$ ). From the values of  $F_{2n}^2$  deduced from a small angle point and a large angle point at the same value of  $q$ , it is possible to determine  $F_{1n}/F_{2n}$  for that value of  $q$ . Since Goldberg has shown that the peak cross section is nearly proportional to the sum of the free neutron and proton cross sections, this value of  $F_{1n}/F_{2n}$  can be found simply by using the Rosenbluth formula and the values of  $F_{2n}^2$  in Fig. 5. If  $Y = F_{1n}/F_{2n}$  and  $R$  is the ratio of  $F_{2n}^2$  for the small angle  $\theta_s$  to that for the large angle  $\theta_L$ , then

The sensitivity of this experiment to  $F_{1n}/F_{2n}$  is low and any limits to be set on  $F_{1n}/F_{2n}$  are rather large.

<sup>18</sup> J. A. McIntyre and R. Hofstadter, Phys. Rev. **98**, 158 (1956); J. A. McIntyre, Phys. Rev. **103**, 1464 (1956); J. A. McIntyre and S. Dhar, Phys. Rev. **106**, 1074 (1957); and J. A. McIntyre and G. R. Bureson, Phys. Rev. **112**, 1155 (1958).

<sup>19</sup> For a summary of the theoretical aspects and experimental results, see L. I. Foldy, Revs. Modern Phys. **30**, 471 (1958).

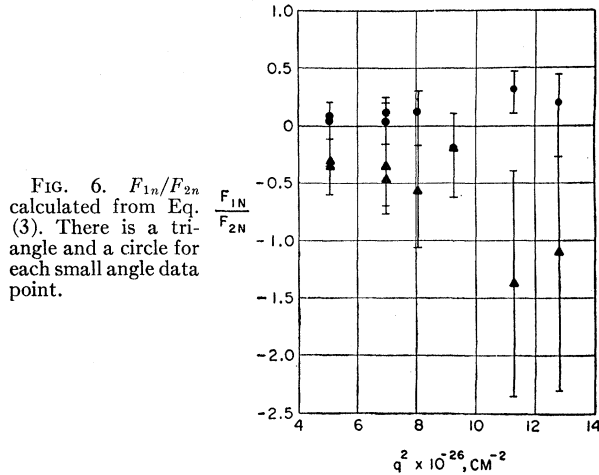


FIG. 6.  $F_{1n}/F_{2n}$  calculated from Eq. (3). There is a triangle and a circle for each small angle data point.

However, the values of  $q$  at which it is possible to make measurements are larger than those of the more sensitive elastic scattering experiments of McIntyre et al.<sup>18</sup> The points of Fig. 6 would not be shifted significantly by a change in the theoretical cross section which was of the order of 5% or less and which was independent of energy and angle or was primarily a function of  $q$  alone. Also, the validity of the assumption that the contributions from  $F_{1n}$  and  $F_{2n}$  to the deuteron peak height have the Rosenbluth angular dependence with negligible error was checked by substituting the measured values of  $F_{1n}/F_{2n}$  back into the complete expression given by Goldberg for the peak cross section and the original data was reproduced.

## VI. CONCLUSIONS

The conclusions to be drawn from the peak-height data are the following:

(a) There is an apparent small difference between  $F_{2n}^2$  and  $F_p^2$  although the difference could be removed if various errors, primarily theoretical, were near their presumed limits.

If the difference is real, the implication is that the apparent nucleon size is not a manifestation of the breakdown of quantum electrodynamics at these distances.

(b) The measured values of  $F_{1n}/F_{2n}$  indicate that for  $q^2 < 12.8 \text{ f}^{-2}$ ,  $F_{1n}/F_{2n}$  lies between limits of +0.5 and -2.5.

## VII. ACKNOWLEDGMENTS

I wish to thank Professor R. Hofstadter for suggesting this experiment and for much inspiration during its course. I am grateful to Dr. R. Herman and the Research Staff of General Motors Corporation for the computations of the Jankus theory. My gratitude is also extended to A. Goldberg for the use of some of his results prior to publication and for his continuing interest; to A. Pittenger for aid in the computer programming; and to the electron scattering group and

the crew of the Mark III linear accelerator for their assistance during this experiment.

## APPENDIX

The Bethe-Heitler formula<sup>20</sup> for the bremsstrahlung cross section leads to the probability that a high-energy electron will lose a fractional energy  $\lambda$  due to emission of a photon while passing through a low- $Z$  medium of thickness  $dx$  cm:

$$w_x(\lambda)d\lambda \cong b\lambda^{-1}(1-\lambda+\frac{3}{4}\lambda^2)d\lambda dx,$$

where  $b$  is a constant depending only on the medium. For a small but finite thickness  $x$ , this expression must be modified to give

$$w_x(\lambda)d\lambda = [\lambda^{bx-1}/\Gamma(bx+1)](bx)(1-\lambda+\frac{3}{4}\lambda^2)d\lambda. \quad (A1)$$

Terms of order  $(bx\lambda)$  and  $(bx\lambda)^2$  have been neglected in this expression, which is deduced by an argument similar to one given by Heitler.<sup>21</sup>

The probability that an electron will lose a fractional energy  $\lambda$  due to photon emission at the time of scattering is calculated, for the case of small  $\lambda$ , from the Schwinger correction<sup>14</sup> to be (in a form analogous to (A1))

$$w_s(\lambda)d\lambda \cong (1+\frac{3}{4}s)/\Gamma(s+1)s\lambda^{s-1}d\lambda. \quad (A2)$$

This expression must be applied twice, for photon emission corresponding to electron energies both before and after scattering. For large  $\lambda$ , an expression for the probability of wide angle bremsstrahlung must be used,<sup>15</sup> i.e.,

$$w_s(\lambda)d\lambda = s\lambda^{-1}(1-\lambda+\frac{1}{2}\lambda^2)d\lambda. \quad (A3)$$

Equations (A2) and (A3) can be incorporated into one as follows:

$$w_s(\lambda)d\lambda = [(1+\frac{3}{4}s)/\Gamma(s+1)]\lambda^{s-1}s(1-\lambda+\frac{1}{2}\lambda^2)d\lambda. \quad (A4)$$

For small  $\lambda$ , this reduces to Eq. (A2) and is equal to Eq. (A3) within a few percent for large  $\lambda$ .

The net probability for a fractional energy loss  $\lambda$  due to radiation both in the target medium and at the time of scattering is then

$$\begin{aligned} w_{xs}(\lambda)d\lambda &= d\lambda \int_0^\lambda w_x(\lambda_1)w_s\left(\frac{\lambda-\lambda_1}{1-\lambda_1}\right)\frac{d\lambda_1}{1-\lambda_1} \\ &= [(1+\frac{3}{4}s)/\Gamma(bx+s+1)]\lambda^{bx+s-1} \\ &\quad \times (bx+s)(1-\lambda+\frac{1}{2}\lambda^2)d\lambda, \end{aligned}$$

where, for simplicity, we have let the coefficient of  $\lambda^2$  in the parentheses of Eq. (A1) be equal to that in Eq. (A4), with negligible error for the conditions of

<sup>20</sup> W. Heitler, *The Quantum Theory of Radiation* (Oxford University Press, New York, 1954), 3rd ed., p. 249. The contribution from the atomic electrons has approximately the same functional form so this is included in the constant  $b$ . See H. A. Bethe and J. Ashkin, *Experimental Nuclear Physics*, edited by E. Segrè (John Wiley & Sons, Inc., New York, 1953), Vol. I, p. 263.

<sup>21</sup> W. Heitler, reference 20, p. 378.

this experiment. Terms similar to those neglected in Eq. (A1) have also been neglected here.

If we let  $w_{ss}(\lambda)d\lambda = w(E_1, E_2)dE_2$ , corresponding to an electron energy  $E_1$  before radiation and  $E_2$  after radiation, then the probability that an electron of initial energy  $E_0$  will have an energy  $E'$  after radiating, scattering, and again radiating will be

$$v(E_0, E')dE' = dE' \int_{E'}^{E_0} \int_{E'}^{E_0} w(E_0, E_1) \times \sigma(E_1, E_2) w'(E_2, E') dE_1 dE_2, \quad (\text{A5})$$

where  $\sigma(E_1, E_2)$  is the theoretical scattering cross section for electrons of initial energy  $E_1$  and final energy  $E_2$  and  $w$  and  $w'$  are the probabilities for radiation before and after scattering, respectively.

For an elastic cross section,  $\sigma(E_1, E_2)$  is a delta function and the integrals of Eq. (A5) can be evaluated approximately to yield Eq. (1) of the text if  $E_4$  in that equation is replaced by  $E_0'$ . Again, terms of the same order as those neglected in Eq. (A1) were neglected in Eq. (1), in addition to terms depending on  $(E_0 - E_3)$  but which were considerably smaller than those that were retained.

If  $\sigma(E_1, E_2)$ , as a theoretical inelastic cross section, is considered to be a series of many delta functions (elastic cross sections), Eq. (2) of the text results, where the summation has been replaced by the integral sign of that expression. In deducing Eq. (2), it was assumed that the shape of  $\sigma(E_1, E_2)$  as a function of  $E_2$  with fixed  $E_1$  does not change with  $E_1$ . This assumption gives adequate accuracy for this work.

## High-Energy Behavior in Quantum Field Theory\*

STEVEN WEINBERG†

*Department of Physics, Columbia University, New York, New York*

(Received May 21, 1959)

An attack is made on the problem of determining the asymptotic behavior at high energies and momenta of the Green's functions of quantum field theory, using new mathematical methods from the theory of real variables. We define a class  $A_n$  of functions of  $n$  real variables, whose asymptotic behavior may be specified in a certain manner by means of certain "asymptotic coefficients." The Feynman integrands of perturbation theory (with energies taken imaginary) belong to such classes. We then prove that if certain conditions on the asymptotic coefficients are satisfied then an integral over  $k$  of the variables converges, and belongs to the class  $A_{n-k}$  with new asymptotic coefficients simply related to the old ones. When applied to perturbation theory this theorem validates the renormalization procedure of Dyson and Salam, proving that the renormalized integrals actually do always converge, and provides a simple rule for calculating the asymptotic behavior of any Green's function to any order of perturbation theory.

### I. INTRODUCTION

IN many respects, the central formal problem of the modern quantum theory of fields is the determination of the asymptotic behavior at high energies and momenta of the Green's functions of the theory, the vacuum expectation values of time-ordered products. Complete knowledge of the asymptotic properties of these functions would allow us to test the renormalizability of a given Lagrangian, to count the number of subtractions that must be performed in dispersion theory, etc. We shall attack this problem from a rather new direction, which allows a solution in perturbation theory, and which provides an analytic tool that may prove useful in solving the problem in the exact theory.

One might hope to find a solution either kinematically, using only assumptions of covariance, causality, etc., or

dynamically, by using the field equations that actually determine the Green's functions. The first method has been successfully applied to the 2-field functions, the particle propagators, and yields the result that the true propagators are asymptotically "larger" than the bare propagators.<sup>1</sup> However, because the theory of several complex variables is so difficult and incomplete, this approach seems unpromising for expectation values of three or more fields. For this reason, and also because we would eventually like to obtain renormalizability conditions on the Lagrangian, we propose to attack the problem on the dynamical level.

Now, what are the equations that, in principle, would determine the Green's functions. In perturbation theory we know that the Green's functions appear as multiple integrals, the integrand being constructed according to the Feynman rules. In a nonperturbative approach the Green's functions are again given by multiple integrals, but with integrands that themselves depend on the

\* Supported in part by the United States Atomic Energy Commission.

† Present address: Lawrence Radiation Laboratory, University of California, Berkeley, California.

<sup>1</sup> H. Lehmann, *Nuovo cimento* **11**, 342 (1954).